

# Two-Dimensional Simulation of Tunneling Using Quantum Lattice-Gas Automata

A. Sakai, Y. Kamakura and K. Taniguchi

Department of Electronics and Information Systems, Osaka University  
2-1 Yamada-oka, Suita, Osaka 565-0871, Japan, sakai@eie.eng.osaka-u.ac.jp

## ABSTRACT

We present two-dimensional (2D) simulation of quantum tunneling across the potential barrier with surface roughness. The impact of the 2D simulation on the transmission coefficient is investigated by comparing the results with 1D simulations. It is also shown that the transmission coefficient depends on the parallel momentum of the incident particle due to the scattering by the surface roughness.

**Keywords:** time-dependent Schrödinger equation, quantum lattice-gas automata, quantum tunneling, surface roughness

## 1 INTRODUCTION

Tunneling current through the ultra-thin gate oxides ( $\sim 1$  nm) is one of the major concerns limiting the scaling of metal-oxide-semiconductor field effect transistors (MOSFETs). In the previous reports, the tunneling currents have been analyzed by assuming uniform gate oxide thicknesses [1], [2]. However, it is known that the Si/SiO<sub>2</sub> interface is not smooth but has a roughness [9], [10], and this would affect the transmission coefficient in particular in the ultra-thin oxide regime.

In this study, to investigate the impact of the surface roughness on the tunneling, we apply the quantum lattice-gas automata (QLGA) method to the analysis of the quantum wave propagation in 2D open systems. We demonstrate the 2D simulations of the transmission coefficient across the rough barrier wall, which is compared to the results of 1D simulations. In addition, we investigate the effect of the parallel momentum of the incident particle on the tunneling across the potential barrier with surface roughness.

## 2 SIMULATION METHOD

### 2.1 Quantum Lattice-Gas Automata

The QLGA has been studied to simulate the time-dependent Schrödinger equation [3]–[7]. It is particularly well suited to implementation on a quantum computer; the many-body quantum system can be simulated very efficiently [5]. On the other hand, its emulation on a classical computer would also have an advantage,

because its unitarity might lead better behavior than standard finite-difference methods [6], [7].

In the QLGA simulation, the space is discretized and two qubits are assigned to each node of the lattice. They contain the probability amplitudes of whether the lattice node is occupied or not by the simulated particles, and the state of the each qubit evolves with time according to a simple cellular automata rule. The effects of an external potential can be easily incorporated by applying a local phase change to the each qubit. The details of the QLGA method are provided in Ref. [7].

In the previous reports on QLGA [5]–[7], the periodic boundary conditions were usually assumed. In order to make this method applicable to the analysis of the open systems, we have recently proposed an algorithm to introduce an absorbing boundary condition; the additional qubit array has been assigned outside the simulation region to store the information about the particles which have flown out from the boundary [8]. Then the QLGA simulation can be used to analyze the electronic wave propagation in the nanoscale devices with open boundary conditions.

### 2.2 Simulated System

Figure 1 schematically illustrates the 2D open system simulated in this study. The potential energy  $V(x, y)$  is set to be  $V_b$  in the barrier region, while  $V = 0$  in the other area. We have considered the surface roughness of the potential barrier wall, whose roughness pattern has been generated randomly assuming the power spectrum density proposed by Pirovano *et al.* [10]:

$$S(q) = \pi \Delta^2 \Lambda^2 \exp \left[ -\frac{(q\Lambda)^4}{4} \right], \quad (1)$$

where  $q$  is the wave number,  $\Delta$  is the roughness r.m.s. value, and  $\Lambda$  is the correlation length. To evaluate the transmission coefficient  $T$  of a quantum particle, the plane wave defined as

$$\Psi_{\text{inj}}(x, y, t) = \exp [i(k_x x + k_y y - \omega t)] , \quad (2)$$

was injected toward the barrier, where  $(k_x, k_y)$  is the wave vector and  $\omega$  is the angular frequency. The energy

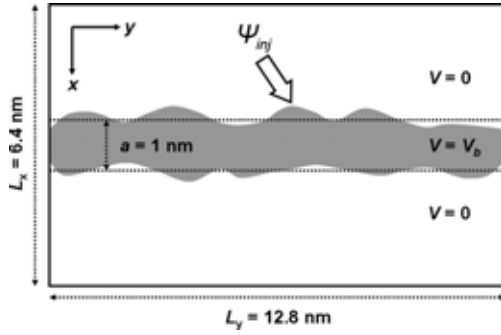


Figure 1: Schematic view of the 2D open systems simulated in this study. The shaded region is the potential barrier.

of the particle is given by

$$E = \hbar\omega = \frac{\hbar^2(k_x^2 + k_y^2)}{2m}, \quad (3)$$

where  $\hbar$  is Planck's constant and  $m$  is the mass of the particle. In this study  $m = 0.3m_0$ , where  $m_0$  is the mass of free electrons, was used to simulate the electrons in Si.

In all the simulations, the field size is set to be 12.8 nm  $\times$  6.4 nm, and the average thickness  $a$  of the barrier wall is 1 nm. The absorbing boundary condition is imposed to the top and bottom boundaries, while along the  $y$  direction the periodic boundary condition is applied.

### 3 RESULTS AND DISCUSSIONS

#### 3.1 Comparison of 1D- and 2D-Tunneling Calculations

Firstly, we investigate the impact of 2D tunneling calculation. As shown in Fig. 2, three calculation methods are compared. In the 1D method (Fig. 2a), the rough interface is flattened and replaced by a flat wall with the same average thickness, and then the  $T$  can be obtained straightforwardly using a 1D tunneling theory. On the other hand, the quasi-2D method shown in Fig. 2b slices the field into narrow sections, and  $T$  is obtained by averaging the 1D transmission coefficients for each section. In this study, these two methods have been compared to the 2D QLGA simulation (Fig. 2c).

Figure 3 shows the calculation results. The quasi-2D model yields larger  $T$  than the 1D calculation. This is because the tunneling probability is significantly enhanced at the spots where the barrier thickness is thinner than  $a$ . Remind that the  $T$  decreases exponentially with the tunneling distance. The quasi-2D method, however, overestimates  $T$  compared to the full 2D calculation. In the 2D model, the incident wave is scattered by the roughness, and the energy component normal to

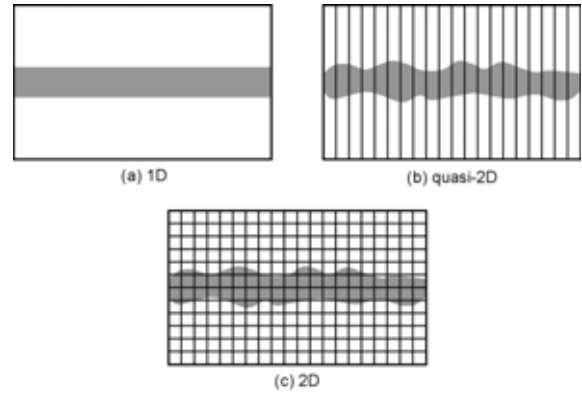


Figure 2: Schematic view of three methods to calculate the  $T$  across the rough barrier. (a) The 1D method replaces the rough wall to a flat one with the same average thickness. (b) The quasi-2D method. The system was sliced into 256 narrow sections. (c) The 2D method. the system was discretized into a 256  $\times$  128 lattice for the QLGA simulation.

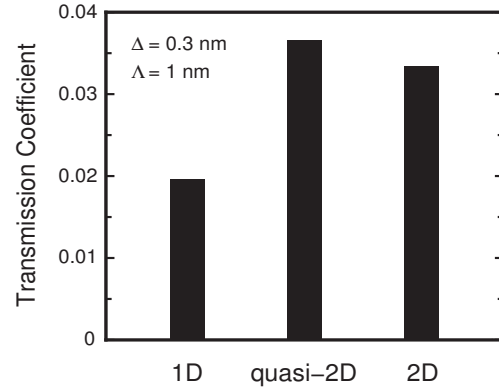


Figure 3: Comparison of  $T$  obtained from three different methods. The particle with  $k_x = 0.8\pi \text{ nm}^{-1}$  and  $k_y = 0$  was injected toward the barrier with  $V_b = 2E$  and  $a = 1$  nm. The roughness of the barrier wall with  $\Delta = 0.3$  nm and  $\Lambda = 1$  nm was considered in quasi-2D and 2D calculations.

the wall, i.e.  $E_x = \hbar k_x^2/2m$ , is partially lost, which causes the reduction of the  $T$ .

#### 3.2 Dependence of Transmission Coefficient on Parallel Momentum

The results of 3.1 indicates that the incident wave is scattered by the surface roughness, which also implies that the parallel momentum of the incident wave could affect the  $T$ . In this section, we investigate the dependence of  $T$  on the parallel momentum  $k_y$  using the 2D QLGA model.

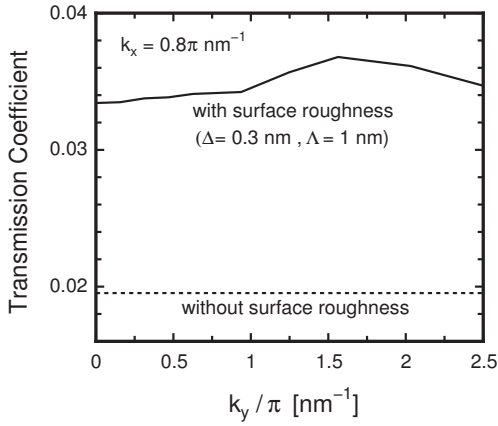


Figure 4: Transmission coefficients across a barrier of  $V_b = 2E_x$  and  $a = 1$  nm plotted as a function of  $k_y$  for the incident plane wave. The  $k_x$  was fixed to  $0.8\pi$  nm $^{-1}$  for all the simulations. The solid and dashed lines are the results for the barrier with and without roughness, respectively.

Figure 4 shows the calculated  $T$  as a function of  $k_y$ . In the case of the flat barrier wall, as is well-known, the  $T$  is independent of  $k_y$ . On the other hand, the simulation results clearly demonstrates that the  $T$  across the rough surface depends on  $k_y$ . A part of the parallel momentum can be transferred to  $k_x$  due to the scattering by the surface roughness, and consequently the  $T$  is considered to be enhanced.

In order to understand this result in more detail, in Fig. 5 we have calculated  $T$  across the barrier with more simple roughness pattern:

$$d(y) = \Delta_s \sin(q_s y) . \quad (4)$$

In the low  $k_y$  region the  $T$  increases with  $k_y$ , and then it decreases in the high  $k_y$  limit. This characteristics also depends on  $q_s$ . In Fig. 6 we show the time evolution for the wave function of  $k_y = 1.4\pi$  nm $^{-1}$ , which exhibits the maximum  $T$ . Note that the incident wave is significantly scattered, and a clear interference pattern is observed in the transmitted wave. The Fourier analysis to the transmitted wave function reveals that it is a superposition of the plane waves with and without scattering. The propagation direction of the scattered wave is tilted by  $\sim 60^\circ$  from the incident wave vector. This is the evidence of the momentum transfer from the parallel to the perpendicular direction due to the scattering. Fig. 7 shows the snap shots for the transmission of the incident plane wave with  $k_y$  of (a)  $0.46\pi$  nm $^{-1}$  and (b)  $3.6\pi$  nm $^{-1}$ , where no enhancement of  $T$  is observed in Fig. 5. Compared with Fig. 6, the scattering of the incident wave is less effective and the interference pattern is not clear, when it is considered that  $k_y$  does not sig-

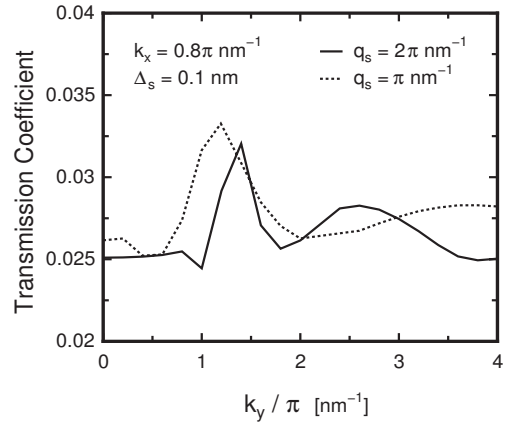


Figure 5: Transmission coefficients across a barrier of  $V_b = 2E_x$  plotted as a function of  $k_y$  for the incident plane wave. The  $k_x$  was fixed to  $0.8\pi$  nm $^{-1}$  for all the simulations. The results for the roughness pattern given by Eq. (4) with  $q_s = \pi$  nm $^{-1}$  (dashed line) and  $2\pi$  nm $^{-1}$  (solid line) are plotted.

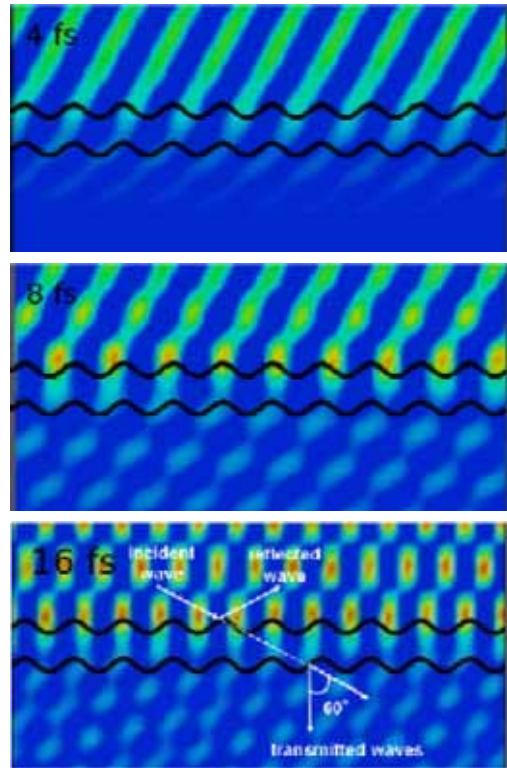
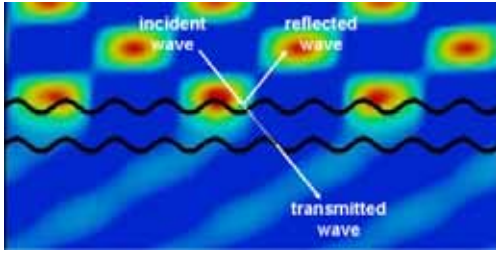
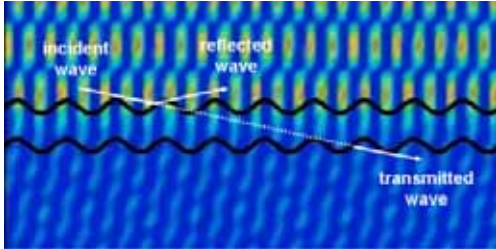


Figure 6: Time evolution of the wave propagation injected toward the barrier with surface roughness. The real part of the wave function is plotted. The parameters used were  $k_x = 0.8\pi$  nm $^{-1}$ ,  $k_y = 1.4\pi$  nm $^{-1}$ ,  $\Delta_s = 0.1$  nm,  $q_s = 2\pi$  nm $^{-1}$ , and  $V_b = 2E_x$ .



(a)



(b)

Figure 7: The snap shots of the wave transmitting across the barrier with surface roughness. The real part of the wave function is plotted. The results for the incident waves with (a) low ( $0.46\pi \text{ nm}^{-1}$ ) and (b) high ( $3.6\pi \text{ nm}^{-1}$ ) parallel momentums are compared. The parameters used were  $k_x = 0.8\pi \text{ nm}^{-1}$ ,  $\Delta_s = 0.1 \text{ nm}$ ,  $q_s = 2\pi \text{ nm}^{-1}$ , and  $V_b = 2E_x$ .

nificantly contribute to the tunneling across the barrier.

## 4 CONCLUSION

We have applied the QLGA simulation to the analysis of the electron tunneling through a potential barrier with the surface roughness. We have compared the three simulation models (1D, quasi-2D, and 2D) and clarified the impact of scattering on the tunneling problem. It has been also demonstrated that the electron transmission coefficient is affected by the parallel momentum. We consider that these effects are not negligible in estimating the tunneling currents in the nanoscale MOSFETs.

## REFERENCES

- [1] M. Stadele, B.R. Tuttle and K. Hess, *J. Appl. Phys.* 89, 348 (2001).
- [2] A. Sakai, A. Ishida, S. Uno, Y. Kamakura and K. Taniguchi, *J. Comp. Electron.* 1, 195 (2002).
- [3] D.A. Meyer, *J. Stat. Phys.* 85, 551 (1996).
- [4] D.A. Meyer, *Phys. Rev. E* 55, 5261 (1997).
- [5] B.M. Boghosian and W. Taylor IV, *Phys. Rev. E* 57, 54 (1998).
- [6] B.M. Boghosian and W. Taylor IV, *Int. J. Mod. Phys. C* 8, 705 (1997).
- [7] J. Yepez and B.M. Boghosian, *Comp. Phys. Comm.* 146, 280 (2002).
- [8] A. Sakai, Y. Kamakura, and K. Taniguchi, submitted for publication.
- [9] S.M. Goodnick, D.K. Ferry and C.W. Wilmsen, *Phys. Rev. B* 32, 8171 (1985).
- [10] A. Pirovano, A.L. Lacaita, G. Zandler, and R. Oberhuber, *Tech. Dig. IEDM*, 527 (1999).